3D Modelling of All-Superconducting Synchronous Electric Machines by the Finite Element Method

Di Hu*[1], Mark D. Ainslie[1], Jin Zou[1] and David A. Cardwell[1]
[1]Department of Engineering, University of Cambridge, Cambridge, UK
*Corresponding author: [1]Bulk Superconductivity Group, Department of Engineering, University of Cambridge, Cambridge, CB2 1PZ, UK, dh455@cam.ac.uk

Abstract: This paper presents the electromagnetic analysis of an all-superconducting synchronous electric machine, focussing on AC loss calculations in high temperature superconducting (HTS) coils. The numerical analyses of two three-dimensional (3D) models are shown, including the model of all-superconducting machine and the model of the HTS stator coils. The models use the ***H***-formulation based on a *B*-dependent critical current density and a bulk approximation, and are implemented using the commercial Finite Element Method (FEM) software package, COMSOL Multiphysics 4.3a. The magnetic boundary conditions for the 3D stator coils are derived from the 3D HTS machine model. The combination of these models allows the estimation of the total AC loss generated in the HTS coils of the all-superconducting machine. Finally, a method to decrease the AC losses of a 3D all-superconducting machine is investigated, which helps improve the efficiency of the machine.

Keywords: AC loss, all-superconducting machine, comsol multiphysics, high-temperature superconductors, numerical analysis, high-temperature superconducting coils

1. Introduction

All-superconducting synchronous electrical machines [1] can achieve higher efficiency and smaller volume than conventional copper-wound machines due to the higher current density of high-temperature superconducting (HTS) materials and their lossless nature for DC current. However, AC losses in the HTS stator windings can be a significant problem for all-superconducting machines, which increase the refrigeration load and therefore reduce the efficiency of the machine [2]. Hence, it is critically important to investigate methods to calculate and decrease the AC losses in the HTS stator of such all-superconducting machines. In [3], it is reported that the use of external flux diverters can help reduce AC loss generated in stacks of tapes. Therefore, it is interesting to investigate the effects of such flux diverters on the AC losses in the HTS stator coils of the machine.

FEM analysis has been applied widely to the simulation of HTS materials, as well as HTS-based devices, to calculate various electromagnetic properties, in order to help predict the performance of practical devices and interpret experimental results. There are three main formulations for FEM calculations: the ***H***-formulation, [4, 5], the ***A-V*** formulation [6, 7] and the ***T- Ω*** formulation [8, 9]. Currently, the ***H***-formulation has become prevalent for HTS material modelling because of its potential for better computational speed and convergence, and ease of implementation.

However, to the best of our knowledge, there is no research on the 3D modelling of all-superconducting machines by use of the ***H***-formulation using commercial FEM software. To promote the development and optimization of all-superconducting machines in the future, a 3D finite element model of an all-superconducting machine is developed based on this formulation in COMSOL Multiphysics 4.3a.

In this paper, the two 3D FEM models are proposed, including a model of the all-superconducting synchronous machine and that for the HTS stator coil. In Section 2, the governing equations for the 3D models are described. The use of COMSOL Multiphysics for the two 3D models, with and without flux diverters, is presented in Section 3. Finally, the average magnetic field seen by the HTS stator coils and the total AC losses of the coils are compared for the all-superconducting machine, with and without flux diverters, and the effects of these diverters on the AC losses are discussed in detail.

2. Governing Equations

As in previous studies [5, 10, 11], the fundamental equations for the 3D HTS model are derived from Maxwell equations and Faraday's (1) and Ampere's (2) laws.

$$\nabla \times \boldsymbol{E} + \mu_0 \mu_r \frac{\mathrm{d}\boldsymbol{H}}{\mathrm{d}t} = 0 \qquad (1)$$

$$\nabla \times \boldsymbol{H} = \boldsymbol{J} \qquad (2)$$

Here, $\boldsymbol{H}$ = (H_x, H_y, H_z) represents the magnetic field, $\boldsymbol{J}$ = (J_x, J_y, J_z) represents the current density, and $\boldsymbol{E}$ = (E_x, E_y, E_z) represents the electric field components. μ_0 is the permeability of free space. For the superconducting layers and air sub-domains, the relative permeability $\mu_r = 1$.

The magnitude of magnetic field, H_{norm}, and the magnitude of the magnetic flux density, B_{norm}, can be calculated by (3) and (4).

$$H_{\text{norm}} = \sqrt{H_x^{\,2} + H_y^{\,2} + H_z^{\,2}} \qquad (3)$$

$$B_{\text{norm}} = \mu_0 \mu_r H_{\text{norm}} \qquad (4)$$

Following [5, 11], the electric field $\boldsymbol{E}$ is assumed to be parallel to current density $\boldsymbol{J}$. The electrical properties of a superconductor can be modelled by an E-J power law [12, 13] as in (5).

$$\boldsymbol{E} = E_0 \left(\frac{\boldsymbol{J}}{J_c}\right)^n \qquad (5)$$

Here, E_0 is the characteristic electric field, 1×10^{-4} V/m, and n = 21. J_c is the critical current density, which varies with the magnitude of the flux density B_{norm}, and is denoted J_c (B_{norm}). The characteristics of measured HTS wire samples can be described by the isotropic relationship (6), as given in [14].

$$J_c(B_{\text{norm}}) = \frac{J_0}{\left(1 + \frac{B_{\text{norm}}}{B_0}\right)^{\beta}} \qquad (6)$$

J_0 represents the critical current density in self-field (i.e., no external field) at 77 K. The specific parameters used in this paper are $J_0 = 2.5 \times 10^{10}$ A/m^2, $B_0 = 0.13$, and $\beta = 0.743$, which are consistent with recent measurement results (to be published) of a short sample of HTS wire at 77 K.

For the non-superconducting regions, a linear Ohm's law is considered, $\boldsymbol{E} = \rho \boldsymbol{J}$, where ρ is a constant resistivity for the specific materials.

The total AC losses Q_{ac} in J/Cycle/m^3 in a superconductor for a period of AC current can be calculated by (7).

$$Q_{\text{ac}} = \frac{1}{V}\int_0^T \mathrm{d}t \int_0^V \boldsymbol{E} \bullet \boldsymbol{J} \mathrm{d}v \qquad (7)$$

Where T is the period, and V is the volume of superconducting material.

Based on [3], strongly magnetic material can work as a flux diverter to help decrease AC loss. For this kind of material, the field magnitude H_{norm} dependence of the relative magnetic permeability should be considered. The following equation (8) expresses the relative permeability $\mu_r(H_{\text{norm}})$ [15].

$$\mu_r(H_{\text{norm}}) = 1 + 1200000\left(1 - \exp\left(-(H_{\text{norm}}/70)^{3.2}\right)\right) H_{\text{norm}}^{\;-0.99} \qquad (8)$$

The hysteretic loss Q_{ferro} in J/Cycle/m^3 for this ferromagnetic material [15] can be calculated by (9).

$$Q_{\text{ferro}}(B_{\max}) = 171.2 B_{\max}^{\;1.344} \quad 0.1 \le B_{\max} \le 1.53 \qquad (9)$$

where $B_{\max}$ represents the maximum magnetic field in the strongly magnetic material. Equation (9) is limited to magnetic fields between 0.1 – 1.53 T, which is an acceptable for the machine application in this paper.

3. Use of COMSOL Multiphysics

The equations governing the model properties described in Section 2 are written in the form of a General Form Partial Differential Equation (PDE) in COMSOL. The model consists of two sub models: the model of the all-superconducting synchronous electrical machine, and the model of the HTS stator coils. The HTS tape is manufactured by SuperPower, and has a critical current of 100 A at 77 K [16]. The width of the conductor is 4 mm and its thickness is 1 µm. For the wound HTS coil, the separation of the HTS tapes is assumed to be 199 µm, to account for other layers in the wire (stabiliser, substrate, and so on) and any insulation layers.

In this paper, the wound coil is approximated as a bulk element to replace the layers of coated conductor in the HTS coils to improve speed and convergence [17]. AC losses are generated when the HTS wire is exposed to a time-varying current or magnetic field [2]. The total AC loss in the HTS coil is composed of the transport AC loss, due to a time-varying current flowing in the coil, and the magnetization AC loss, due to a time-varying varying external magnetic field [1]. The bulk approximation tends to overestimate transport loss and underestimate magnetization

loss. However, the total AC loss calculation compared to real thickness and analytical models is reasonably small [18]. For the bulk approximation, the integration of the current density in each bulk element is equal to the applied current I in the tape multiplied by the number of turns N.

Dirichlet boundary conditions can be applied to model an externally applied magnetic field in different directions. Neumann boundary conditions are applied to describe the continuity between the air and superconductor sub-domains.

Integral constraints can be applied to describe the particular transport current in the HTS coil. A transport current I_t flowing through any surface s can be described by (10).

$$I_t = \int J \cdot \mathrm{d}s_t \qquad (10)$$

where s_t represents the surface differential element normal to the cross-section of the coil.

Following [11], a swept mesh is applied to these two 3D models to keep the total number of degrees of freedom at a reasonable level.

3.1 3D Synchronous Motor Model

The model of the 3D HTS synchronous machine is simulated first. For this all-superconducting machine, an air core is preferred to avoid iron saturation, hysteresis and excessive heating [19], and HTS coils are considered for both the stator and rotor windings. All coils are modelled using the bulk approximation. Based on [20], the apparent output power for an HTS electrical machine is proportional to the peak value of the fundamental component of flux density at the armature winding. Because of the limitation of the critical current (100 A) of the HTS wire, the applied DC current is assumed to be 80 A for the field coils in the rotor. Since no externally applied magnetic field exists, the Dirichlet boundary conditions are set as $H_n = 0$, where n = x, y, z for a sufficiently large air subdomain in the HTS machine model. The specific parameters for 3D machine are presented in Table 1. The geometry and magnetic field distribution of the all-superconducting machine are shown in Figure 1. The air gap of this HTS machine is very small and therefore is not shown.

Table 1: Motor Parameters.

PARAMETERS	SYMBOL	VALUE
Pole-pairs	p	2
Phase number	m	3
Rotor radius	R_r	130 mm
Field winding coil turns (rotor)	N_r	300
Field winding coil thickness (rotor)	h_r	9 mm
Field winding coil width (rotor)	w_r	30 mm
Distance between field coil sides (rotor)	W_r	106 mm
Armature winding position radius	R_s	153 mm
Armature winding coil turns (stator)	N_s	110
Armature winding coil thickness (Stator)	h_s	9 mm
Armature winding coil width (Stator)	w_s	11 mm
HTS wire critical current (77 K, self-field)	I_c	100 A
Operating temperature	T_{op}	77 K
Motor length	L	300 mm

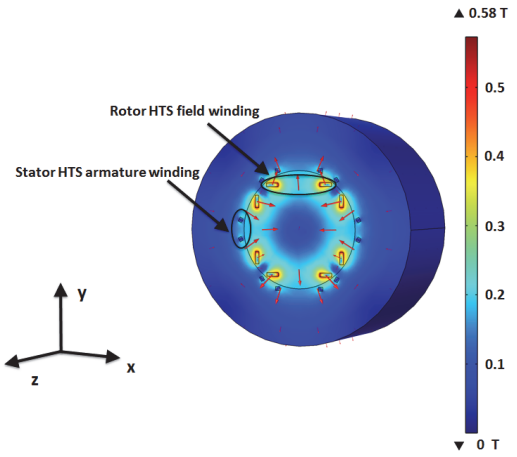

Figure 1. The 3-D geometry and magnetic field distribution of the all-superconducting machine.

3.2 3D HTS Stator Coil Model

The magnetic boundary conditions for the 3D stator coil model are derived from the 3D HTS machine. To be precise, the Dirichlet boundary condition of magnetic fields H_x, H_y, H_z, was applied to represent the external magnetic field seen by the stator coil from the rotor field. The geometry of the HTS coil of 110 turns is modelled by a bulk element 11 mm wide by 9 mm high, and 300 mm in length, which is consistent with Table 1. An AC current of frequency 50 Hz and magnitude 40 A is applied to the stator's armature coils. The 3D HTS coil model with the bulk approximation is presented in Figure 2. Because of symmetry, only one side of the HTS coil is shown in Figure 2.

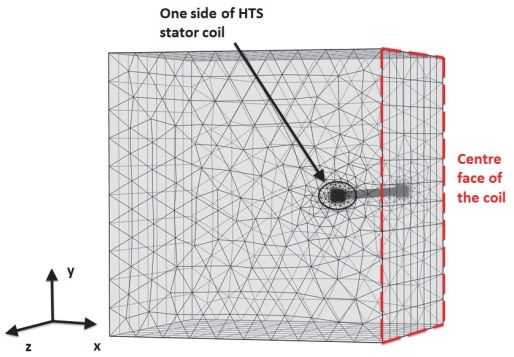

Figure 2. Geometry of the HTS stator coil model using the bulk approximation.

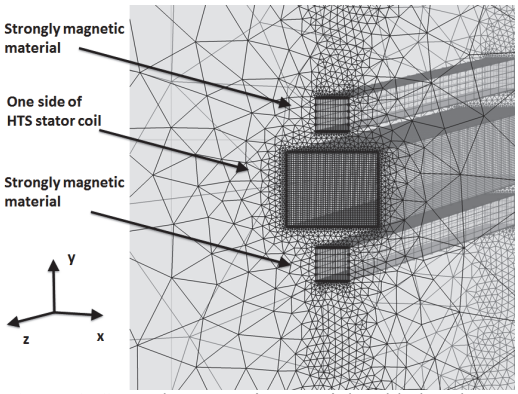

Figure 3. Strongly magnetic materials added at the top and the bottom of the HTS coil for diverting flux.

Using (7), combining the two models can help estimate the total AC losses of the HTS stator coils.

3.3 Use of Flux Diverters

Finally, magnetic materials were added to the coil model and all-superconducting synchronous machine model to divert flux. Ferromagnetic covers were placed on the edges of the superconducting tapes in the stack as seen looking at the cross-section of the coils. Strongly magnetic materials 4 mm wide by 4 mm high and of length 300 mm were added at the top and the bottom of the HTS coil to divert flux, as shown in Figure 3. There was a 3 mm gap between the magnetic material and the HTS stator coil, which represents the thickness of the coil former and the insulation layer. By symmetry, only one side of the HTS coil is shown in Figure 3.

From Figure 3, the width of the flux diverter is shorter than the width of the HTS coil. The main reason is that flux diverter can increase the local field at the edge of the flux diverter. If the width of the flux diverter is the same as that of HTS coil, the innermost turn will see a relatively higher local magnetic field, which will decrease the local critical current in this region and therefore decrease the critical current of the whole coil [21, 22]. In order to avoid this situation, the width of the flux diverter is shorter than that of the HTS coil. The effects of the flux diverter on AC loss reduction will be analysed comprehensively.

4. Results

In this section, the two models – without and with flux diverters - are considered as Models 1 and 2. Based on the all-superconducting synchronous machine model, a comparison of the magnitude of the external magnetic fields, B_{norm}, seen by the stator with and without flux diverters, is shown in Figure 4. These magnetic fields are calculated when the rotor in Figure 1 rotates through 180°. Again, because of symmetry, the same rotating field will exist between 180° and 360°. For this synchronous machine, the frequency of the applied current in the HTS stator model is 50 Hz and therefore the rotating speed of the all-superconducting machine is 1500 rpm. The time taken for the rotor to rotate half a revolution (180°) is 20 ms.

From Figure 4, it can be seen that the flux diverters can help decrease the magnitude of the average external magnetic field, B_{norm}, seen by the stator in the all-superconducting machine. This arises from the fact that the flux diverters attract magnetic flux towards them [3], resulting in less penetration of magnetic flux lines into the superconducting material.

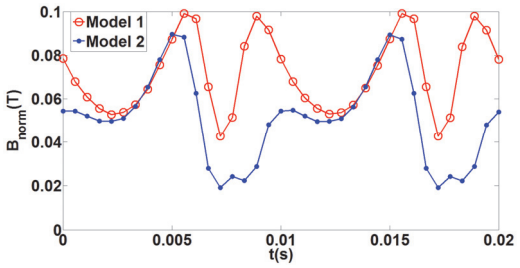

Figure 4. Magnitude of the magnetic field, B_{norm}, seen by the stator coil as the rotor rotates from its initial position through 180° (half a revolution).

In order to investigate the effects of the flux diverters further, a comparison of the AC losses of a single HTS stator coil, with and without flux diverters, is shown in Table 2. For the external magnetic field shown in Figure 4, the magnitude of the applied current in the coil is 40 A. Considering the coil has 110 turns, the total current flowing in the bulk element is 4400 A. For the HTS coil, the AC losses consist of the magnetization loss and transport loss, which are calculated separately in Table 3. The calculation comes from (7) and (9). Considering the specific volumes of the different materials, the AC losses per stator coil are presented in J/Cycle.

Table 2: AC loss comparison of a single HTS stator coil with and without flux diverters.

	Model 1	Model 2
Magnetization loss	296 J/cycle	276 J/cycle
Transport loss	765 J/cycle	720 J/cycle
Ferromagnetic material loss	0 J/cycle	3.8×10^{-3} J/cycle

From Table 2, it can be seen that the flux diverter can help decrease the magnetization loss, because the flux diverters help decrease the external magnetic field seen by the stator coil. The flux diverters can also help decrease the transport loss, because the diverters attract magnetic flux lines out of the superconducting material, which is consistent with [3]. Although the ferromagnetic material has a hysteretic loss, this can be ignored in comparison with the AC losses in the HTS material. In summary, the flux diverters can help decrease both the magnetization and transport losses in the HTS coils, which can help improve the efficiency of the machine.

In the future, further development of the model is required in terms of the all-superconducting machine design. Coil optimisation and the optimisation of air gap magnetic field are needed, leading to further investigation of the machine's performance with such flux diverters.

5. Conclusions

In this paper, 3D numerical analysis of an all-superconducting machine and its constituent HTS coils, were carried out using the ***H***-formulation and a bulk approximation, which allows a completely integrated 3D model, including both the electromagnetic properties of the superconductor and motor, to be developed. The methods of calculating and decreasing the AC losses of a 3D all-superconducting machine awee investigated, which allows improvements

in the efficiency of the machine. Based on the simulation results, it is found that flux diverters can help decrease the external magnetic field seen by the stator coils of the machine. Furthermore, the flux diverters can help decrease both the magnetization and transport AC losses, which allows the total AC loss in the HTS coils to be decreased and the machine efficiency to be improved significantly.

6. References

1. M. D. Ainslie *et al*, "Numerical analysis and finite element modelling of an HTS synchronous motor", *Physica C*, **vol. 47**, pp. 1752 (2011)
2. D. Hu, M. D. Ainslie, J. Zou, and D. A. Cardwell, "Numerical Analysis of Non-Uniformities and Anisotropy in High Temperature Superconducting (HTS) Coils", submitted for publication
3. M. D. Ainslie *et al*, "Numerical Analysis of AC Loss Reduction in HTS Superconducting Coils Using Magnetic Materials to Divert Flux", *IEEE Trans. Appl. Supercond.*, **vol. 23**, pp. 470014 (2013)
4. M. D. Ainslie *et al*, "Comparison of first- and second-order 2D finite element models for calculating AC loss in high temperature superconductor coated conductors", *Int. J. Comput. Math. Electr. Electron. Eng.*, **vol. 30**, pp. 762 (2011)
5. M. Zhang and T. A. Coombs, "3D modelling of high- T_c superconductors by finite element software", *Supercond. Sci. Technol.*, **vol. 25**, pp. 015009 (2012)
6. L. Prigozhin, "Analysis of critical-state problems in type-II superconductivity", *IEEE Trans. Appl. Supercond.* **vol. 7**, pp. 3866 (1997).
7. A. M. Campbell, "A direct method for obtaining the critical state in two and three dimensions", *Supercond. Sci. Technol.*, **vol. 22**, pp. 034005 (2009)
8. N. Amemiya *et al*, "Numerical modelings of superconducting wires for AC loss calculations", *Physica C*, **vol. 310**, pp. 16 (1998)
9. G. Meunier *et al*, "A nonlinear circuit coupled t-t_0-φ formulation for solid conductors", *IEEE Trans. Magn.*, **vol.39**, pp. 1729 (2003)
10. V. M. Rodriguez- Zermeno, F. Grilli, and F. Sirois, "A full 3D time-dependent electromagnetic model for Roebel cables", *Supercond. Sci. Technol.*, **vol. 26**, pp. 052001 (2013)
11. F. Grilli, R. Brambilla, F. Sirois, A. Stenvall, S. Memiaghe, "Development of a three-dimensional finite-element model for high-temperature superconductors based on *H*-formulation", *Cryogenics*, **vol. 53**, pp. 142 (2013)
12. J. Rhyner, "Magnetic properties and AC-losses of superconductors with power law current-voltage characteristics", *Physica C*, **vol. 212**, pp. 292 (1993)
13. C. J. G. Plummer, and J. E. Evetts, "Dependence of the shape of the resistive transition on composite inhomogeneity in multifilamentary wires", *IEEE Trans. Magn.*,**vol. 23**, pp. 1179 (1987)
14. E. Pardo, and F. Grilli, "Numerical simulations of the angular dependence of magnetization AC losses coated conductors, Roebel cables and double pancake coils", submitted for publication", *Supercond. Sci. Technol.*, **vol. 25**, pp. 014008 (2012)
15. M. D. Ainslie, T. J. Flack, A. M. Campbell, "Calculating transport AC losses in stacks of high temperature superconductor coated conductors with magnetic substrates using FEM", *Physica C*, **vol. 472**, pp. 50 (2012)
16. http://www.superpower-inc.com/ [online]
17. M. D. Ainslie *et al*, "Modeling and Electrical Measurement of Transport AC Loss in HTS-Based Superconducting Coils for Electric Machines", *IEEE Trans. Appl. Supercond.,* **vol. 21**, pp. 3265 (2010)
18. F. Grilli, and S. P. Ashworth, "Quantifying AC Losses in YBCO Coated Conductor Coils", *IEEE Trans. Appl. Supercond.*, **vol. 17**, pp. 3187 (2007)
19. H-W. Neumüller *et al*, "Advances in and prospects for development of high-temperature superconductor rotating machines at Siemens", *Supercond. Sci. Technol.*, **vol. 19**, S114 (2006)
20. J. R. Bumby, "Superconducting Rotating Electrical Machines", Oxford: Clarendon, pp. 71-74 (1983)
21. M. D. Ainslie, D. Hu, J. Zou, D. A. Cardwell, "Simulating and Improving the In-Field Performance of High-Temperature Superconducting Coils", submitted for publication
22. M. Zhang *et al*, "Study of second generation, high-temperature superconducting coils: Determination of critical current," *J. Appl. Phys*., **vol. 111**, pp. 083092 (2012)

7. Acknowledgements

The work of Di Hu and Jin Zou was supported by Churchill College, the China Scholarship Council and the Cambridge Commonwealth, European and International Trust. The work of Mark Ainslie was supported by a Royal Academy of Engineering Research Fellowship.